Mobius3D

The complete patient QA system

3D patient plan QA

3D IMRT/VMAT pre-treatment QA

3D in vivo daily treatment QA

Online patient positioning QA

Upgrade your patient safety by bridging the gap between patient QA and machine QA

DoseLab® machine QA software, the complete TG-142 solution, is now integrated into the Mobius3D® patient QA system!

Visit mobiusmed.com/mobius3d to learn more.

Safety information: Radiation may cause side effects and may not be appropriate for all cancers.

varian | MOBIUS

Dosimetric characterization of a new directional low-dose rate brachytherapy source

Manik Aima,[1,*] Larry A. DeWerd,[1] Michael G. Mitch,[2]
Clifford G. Hammer,[1] and Wesley S. Culberson[1]

[1]*Department of Medical Physics, School of Medicine and Public Health, University of Wisconsin-Madison, Madison, Wisconsin 53705*

[2]*National Institute of Standards and Technology, Gaithersburg, MD, 20899*

(Dated: March 11th 2018)

Abstract

Purpose: CivaTech Oncology Inc. (Durham, NC) has developed a novel low-dose rate (LDR) brachytherapy source called the CivaSheet.™ The source is a planar array of discrete elements ("CivaDots") which are directional in nature. The CivaDot geometry and design are considerably different than conventional LDR cylindrically symmetric sources. Thus, a thorough investigation is required to ascertain the dosimetric characteristics of the source. This work investigates the repeatability and reproducibility of a primary source strength standard for the CivaDot, and characterizes the CivaDot dose distribution by performing in-phantom measurements and Monte Carlo (MC) simulations. Existing dosimetric formalisms were adapted to accommodate a directional source, and other distinguishing characteristics including the presence of gold shield x-ray fluorescence were addressed in this investigation.

Methods: Primary air-kerma strength (S_K) measurements of the CivaDots were performed using two free-air chambers namely, the Variable-Aperture Free-Air Chamber (VAFAC) at the University of Wisconsin Medical Radiation Research Center (UWMRRC), and the National Institute of Standards and Technology (NIST) Wide-Angle Free-Air Chamber (WAFAC). An inter-comparison of the two free-air chamber measurements was performed along with a comparison of the different assumed CivaDot energy spectra and associated correction factors. Dose distribution measurements of the source were performed in a custom polymethylmethacrylate (PMMA) phantom using Gafchromic™ EBT3 film and thermoluminescent dosimeter (TLD) microcubes. Monte Carlo simulations of the source and the measurement setup were performed using MCNP6 radiation transport code.

Results: The CivaDot S_K was determined using the two free-air chambers for eight sources with an agreement of better than 1.1% for all sources. The NIST measured CivaDot energy spectrum intensity peaks were within 1.8% of the MC-predicted spectrum intensity peaks. The difference in the net source-specific correction factor determined for the CivaDot free-air chamber measurements for the NIST WAFAC and UW VAFAC was 0.7%. The dose-rate constant analog was determined to be 0.555 cGy h^{-1} U^{-1}. The average difference observed in the estimated CivaDot dose-rate constant analog using measurements and MCNP6 predicted value (0.558 cGy h^{-1} U^{-1}) was 0.6% ± 2.3% for eight CivaDot sources using EBT3 film, and -2.6% ± 1.7% using TLD micro-cube measurements. The CivaDot 2-D dose-to-water distribution measured in phantom was compared

to the corresponding MC predictions at six depths. The observed difference using a pixel-by-pixel subtraction map of the measured and the predicted dose-to-water distribution were generally within 2% to 3%, with maximum differences up to 5% of the dose prescribed at the depth of 1 cm.

Conclusion: Primary S_K measurements of the CivaDot demonstrated good repeatability and reproducibility of the free-air chamber measurements. Measurements of the CivaDot dose distribution using the EBT3 film stack phantom, and its subsequent comparison to Monte Carlo predicted dose distributions were encouraging, given the overall uncertainties. This work will aid in the eventual realization of a clinically viable dosimetric framework for the CivaSheet based on the CivaDot dose distribution.

Keywords: Brachytherapy, dosimetry, directional sources, TG-43, EBT3 film

I. INTRODUCTION

Brachytherapy is an advanced radiotherapy modality that includes use of radioactive sources for cancer treatments. For low-dose rate (LDR) brachytherapy, numerous low-energy photon-emitting sources (commonly ^{125}I or ^{103}Pd) have been used for treatment. The American Association of Physicists in Medicine (AAPM) Task Group No. 43 report (TG-43) and its associated updates [1–3] recommended a formalism to characterize these sources, and described the relevant dosimetric parameters in detail. There have been advances in source geometry and design since the publication of the report [4–8] to improve upon the conformity of the delivered dosimetric distributions, such as the CivaString™, OptiSeed™, RadioCoil™ and SmartSeed™ brachytherapy sources.

A novel LDR brachytherapy source has been developed by CivaTech Oncology, Inc (Durham, NC) called the CivaSheet.™ The CivaSheet is a planar source array consisting of discrete ^{103}Pd source elements called the CivaDots which are directional in nature. A gold shield is present in each CivaDot in close proximity to the active source region, imparting directionality to the radiation output of the device. A directional source can potentially improve the therapeutic ratio for a given brachytherapy treatment when compared

* aima@wisc.edu

Disclaimer: Certain commercial equipment, instruments, or materials are identified in this paper to foster understanding. Such identification does not imply recommendation or endorsement by NIST or UW, nor does it imply that the materials or equipment identified are necessarily the best available for the purpose.

to conventional sources, by selectively targeting diseased tissue and sparing the surrounding healthy structures. Previous investigations [9, 10] reported reduction in dose to normal tissue in breast and prostate cancer treatments when comparing directional to conventional interstitial sources. The manufacturer, CivaTech Oncology, has been developing the device and investigating its efficacy for pancreatic, abdomino-pelvic, and colorectal cancer treatments (trials NCT03109041, NCT02843945, NCT02902107) amongst other sites.

The CivaSheet is unique in design and varies significantly from conventional LDR brachytherapy sources, and therefore, a thorough investigation needs to be performed to ascertain the dosimetric characteristics of the device prior to its clinical use. For conventional LDR sources, guidelines and dosimetric formalisms have been recommended by the AAPM. [2, 11–13] There is currently no standard protocol for calibration or quality assurance of planar or directional LDR sources. The existing TG-43 formalism needs to be adapted to accommodate the directional CivaDot source. Previous work by Aima et al. [14] addressed the source strength determination for a CivaDot by performing primary air-kerma strength (S_{K}) measurements. Rivard [15] published the CivaDot dose distribution results as predicted by Monte Carlo simulations. Cohen et al.[16] investigated the suitability of Rivard's results for clinical commissioning of the CivaSheet. This work aims to help in the dosimetric characterization of the CivaDot by performing in-phantom measurements and Monte Carlo simulations as well as investigate the repeatability and reproducibility of the source strength standard for the CivaDot.

An inter-comparison of two free-air chambers was performed, namely, the University of Wisconsin Variable-Aperture Free-Air Chamber (UW VAFAC) [17] which is a research instrument, and the National Institute of Standards and Technology Wide-Angle Free-Air Chamber (NIST WAFAC) [18], which is the U.S. primary standard for S_{K} determination of low-energy photon-emitting LDR sources. The inter-comparison was performed to facilitate the establishment of a national primary source-strength standard for the CivaDot. Previous primary S_{K} measurements have been performed using the UW VAFAC.[4, 14, 17, 19] The air-kerma strength definition as recommended by TG-43 protocol was adapted to accommodate directional sources as reported previously.[14] The inter-comparison consisted of three investigations, first, comparing the NIST-measured CivaDot energy spectrum to the UW-predicted spectrum, second, contrast the CivaDot source-specific correction factors for the two free-air chambers, and finally, compare the S_{K} determined for eight CivaDot sources.

This work proposes an element-based approach to characterize the CivaSheet dose distribution, in accordance with previous work by Colonias et al. [20] and Yang et al. [21] for conventional ^{125}I and ^{131}Cs source arrays. In order to do so, the dosimetric characterization of a CivaDot needs to be performed. An investigation was conducted to study the dose distribution of the source in phantom. The dose-rate constant analog for the CivaDot was determined using thermoluminescent dosimeters and Gafchromic EBT3 film in a polymethylmethacrylate (PMMA) phantom. Another experiment was performed with a stack of EBT3 films placed in a custom PMMA phantom to study the CivaDot dose distribution at different depths. The CivaDot source along with the experimental setup was modeled in the Monte Carlo n-Particle Transport Code 6 v1.0 (MCNP6) and simulations were performed to generate various correction factors and provide a comparative basis for the measurements. The purpose of this work is thus to ascertain the dosimetric characteristics of a new directional LDR brachytherapy source called the CivaDot using a variety of measurements and Monte Carlo simulations.

II. METHODS AND MATERIALS

A. Source description

The CivaDot source is comprised of a cylindrical organic polymer capsule encased within a bioabsorbable membrane. The polymer capsule consists of a ^{103}Pd region, a gold shield (which helps define the 'hot' and the 'cold' side of the device), and is sealed with epoxy. Figure 1a is an illustration of the CivaDot which has been adapted from Aima et. al, [14] accounting for a slight change in the bioabsorbale membrane orientation. The CivaSheet, and other CivaDot specifications have been published in previous works. [14, 15] For this work, the reference plane was defined as the bottom of the palladium region in the device and the origin was defined as the intersection of the reference plane and the cylindrical axis of the CivaDot. Figure 1b is an illustration of the coordinate system used for CivaDot dosimetry for this work.

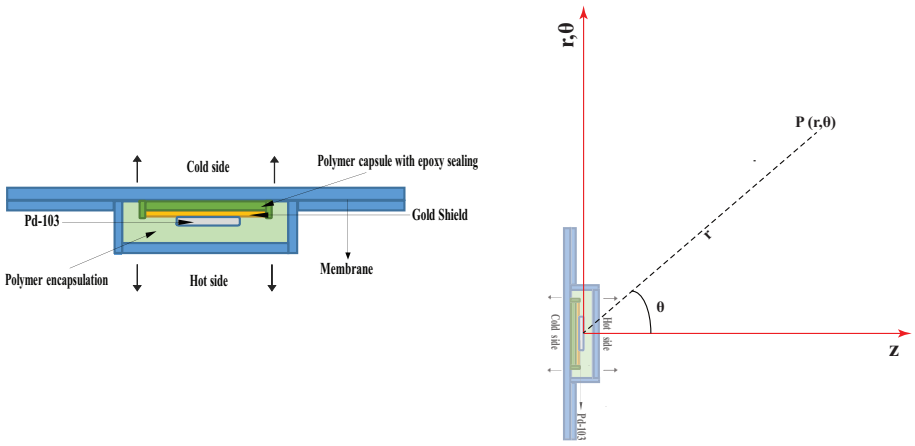

(a) (b)

FIG. 1: a. An illustration of the CivaDot with its components in a cross-sectional view. Figure 1a has been adapted from Aima et al. [14] b. An illustration of the coordinate system for CivaDot dosimetry. Please note that the figures are not to scale.

Adapted TG-43 parameters

Nath et al. and Rivard et al. [1–3] established a formalism for the dosimetric characterization of conventional LDR brachytherapy sources. These traditional sources were cylindrically symmetric and had isotropic azimuthal emission. The TG-43 report proposed the following dosimetric formalism:

$$\dot{D}(r,\theta) = S_{\mathrm{K}} \cdot \Lambda \cdot \frac{G_X(r,\theta)}{G_X(r_0,\theta_0)} \cdot g_X(r) \cdot F(r,\theta), \tag{1}$$

where $\dot{D}(r,\theta)$ is the absorbed dose-rate-to-water in water at distance r and angle θ from the source, S_{K} is air-kerma strength of the source, measured as the averaged source strength on the transverse axis of the source in vacuo at 1 meter, Λ is the dose-rate constant, defined as the ratio of absorbed dose-rate-to-water at 1 cm to the S_{K} on the transverse axis of the source, and $G_X(r,\theta)$, $g_X(r)$, $F(r,\theta)$ are the geometric, radial, and 2D anisotropy function, respectively.

In the case of the CivaDot, the directional as well as planar nature of the source array renders the direct application of the TG-43 protocol inappropriate. The definitions of S_{K}, Λ, $G_X(r,\theta)$, $g_X(r)$, and $F(r,\theta)$ were adapted to accommodate this source, and analogous

dosimetric parameters were defined for the source. CivaDot S_{K} was defined as a static on-axis (source cylindrical axis) measurement,[14] Λ, $G_X(r,\theta)$, $g_X(r)$, and $F(r,\theta)$ were all defined on the source cylindrical axis considering the directionality of the CivaDot. A point source was assumed for the geometry function.

B. Monte Carlo simulations

The CivaDot was modeled in the Monte Carlo transport code MCNP6 [22] using source details including material specifications, device dimensions and schematics provided by CivaTech Oncology. The source was simulated in various geometries including:

- A full UW VAFAC model with the CivaDot in its measurement position
- The source in a PMMA phantom with (a) TLD microcubes, (b) EBT3 film
- The source in a PMMA phantom with an EBT3 filmstack phantom
- The source in a water phantom

The updated low-energy photon cross section data library (mcplib12) was used for the simulations. The ^{103}Pd photon spectrum from the National Nuclear Data Center online NUDAT 2.6 database [23] was used. A *F4 tally [22] was used for absorbed-dose calculations, with energy fluence modified by μ_{en}/ρ values. The modified *F4 tally is a collision kerma tally and can be used as an approximation for the absorbed dose. [2] A minimum of 10^9 histories were used for each simulation. The dosimeters were modeled as per manufacturer's specifications, and photon mass-energy absorption cross-sections were used from the NIST XCOM database.[24] The photon transport cut off was set to 100 eV. As described in the previous publication [14], the amount of ^{103}Pd material present in the active palladium region of the source can be of variable loading based on the specific activity of the material available and the prescription dose. This was referred to as palladium loading. All Monte Carlo simulations for this work assume a palladium loading of 50%, i.e. the ^{103}Pd region is uniformly filled with 50% palladium material and 50% epoxy by mass, with a net density of $\rho = 1.9987\,\mathrm{g\,cm^{-3}}$. The variation in calculated results due to palladium loading is addressed in the uncertainty section.

C. Primary S_K measurements and free-air chamber inter-comparison

The UW VAFAC is a research instrument at the University of Wisconsin-Madison. It is a large-volume free-air chamber that has been used to perform primary S_K measurements of various photon-emitting LDR brachytherapy sources.[4, 14, 17, 19] The CivaDot measurement setup when using the UW VAFAC was explained in detail by Aima et al.[14] The UW VAFAC has five interchangeable brass aperture sizes. This work used the UW VAFAC Aperture No. 2 which collimates the radiation emitted from the source into a cone with a half angle of 7.6°. This aperture has the same collimating solid angle as the NIST WAFAC aperture, which was the other free-air chamber used in this study. The NIST WAFAC is the U.S. national primary standard for low-energy photon-emitting brachytherapy sources.[18] Both free-air chamber measurements were performed with the CivaDot held in a static holder and the source cylindrical axis transverse to the aperture plane (hot side of the source facing the primary aperture). An inter-comparison of the CivaDot primary S_K determination was performed using the two free-air chambers for eight CivaDot sources. This inter-comparison provides us with an estimation of the repeatability and reproducibility of the CivaDot S_K measurements.

1. CivaDot energy spectrum comparison

As reported previously, [14] the presence of a gold shield (in close proximity to the radioactive part of the source) alters the energy spectrum of the CivaDot in comparison to conventional LDR ^{103}Pd brachytherapy sources. For the purpose of S_K determination, NIST measures the source energy spectrum using a high-purity germanium detector with appropriate detector response correction factors. This measured spectrum was compared to UW calculated CivaDot energy spectrum using MCNP6 simulations assuming a palladium loading of 50%. Since the Monte Carlo resolution is higher than the detector resolution, the MC predicted spectrum was consolidated into energy bins corresponding to the NIST measured spectrum. A comparison of the spectra was performed and the presence of the gold fluorescence was investigated.

2. CivaDot source-specific correction factors for free-air chamber measurements

The CivaDot source-specific correction factors were also compared for the two free-air chambers. A detailed description of the correction factors that need to be determined for the free-air chambers was given by Seltzer et al.[18] and Culberson et al.[17] NIST determines the correction factors for the WAFAC using a combination of empirical, analytical and MC methods as described by Seltzer et al.[18] For the UW VAFAC, the correction factors were calculated for Aperture No. 2 using Monte Carlo methods (MCNP6 code) as outlined by Culberson et al. and Aima et al.[14, 17] Though these are two different free-air chambers, the comparison provides a good accuracy check for the corrections as the methods used are completely different and are both sensitive to low-energy gold fluorescence observed in the CivaDot energy spectrum.

3. Primary S_K measurements performed without the presence of an aluminum filter

The use of an aluminum filter when performing a primary S_{K} measurement was recommended by the TG-43 report [2] to exclude the titanium fluorescence present in conventional LDR sources. However, the CivaDot does not contain a titanium encapsulation and the magnitude of the correction for the aluminum filter attenuation, k_{foil}, is sensitive to the the low-energy photons which includes the fluorescence observed from the gold shield. An additional investigation was performed with the UW VAFAC to study the impact of the aluminum filter on the CivaDot S_{K} determination. The aluminum filter was removed from the UW VAFAC, and CivaDot S_{K} measurements were performed. These measurements were compared to NIST-determined S_{K} values for the same sources using the WAFAC with the presence of an aluminum filter.

D. Dose-rate constant analog determination

A polymethyl methacrylate (PMMA) phantom was designed to perform dose-to-water measurements of the CivaDot using thermoluminescent dosimeter micro-cubes (TLDs) and Gafchromic EBT3 films manufactured by Ashland Inc. (Convington, KY). Figure 2 illustrates the PMMA phantom design for measuring the dose-rate constant (DRC) analog for the CivaDot using TLDs. These measurements were performed in a PMMA phantom of

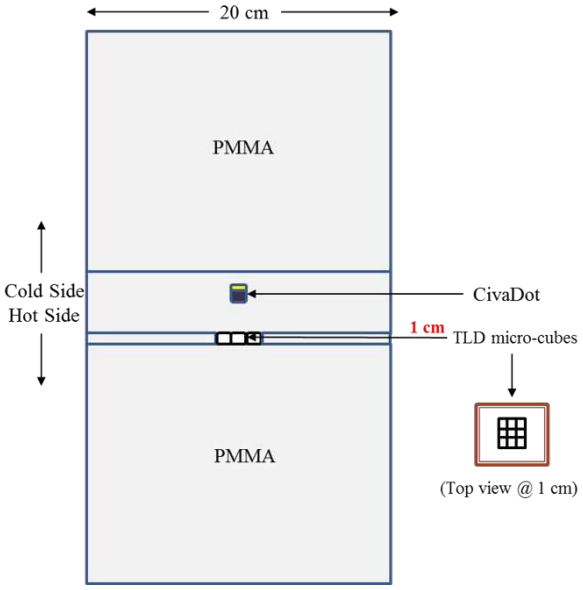

FIG. 2: Illustrations of the PMMA phantom used for the CivaDot DRC analog measurement using nine TLD micro-cubes in a $3 \times 3 \times 1$ mm^3 slot centered on the source cylindrical axis at 1 cm (red label) away from the source. A smaller figure on the side (Top view @ 1cm) is provided as an illustration of the top view of the TLD microcubes (black) placed side-by-side in the relevant PMMA insert (red) at 1 cm plane. Please note that the illustrations are not to scale.

dimensions $20 \times 20 \times 12$ cm^3. The TLD micro-cubes used were TLD-100 model (LiF:Mg,Ti) manufactured by Thermo Fisher Scientific Inc. (Waltham, MA). The source was placed in the center of the phantom, and nine TLD micro-cubes were irradiated along its central axis at a distance of 1 cm on the hot side of the source. The nine TLD micro-cubes were placed side-by-side in a $3 \times 3 \times 1$ mm^3 slot in the phantom, which was centered on the source long axis. For conventional brachytherapy sources, this measurement is usually performed on the source transverse axis. Dose-to-water measurements were also performed using an EBT3 film for five CivaDot sources in the PMMA phantom using a different insert. The EBT3 film was placed on top of a PMMA slab and the film edges were secured using kapton tape. The setup was similar to the TLD measurements, with a 3×3 cm^2 segment of EBT3 film placed at 1 cm away from the source along its central axis.

1. TLD microcubes

TLDs were annealed using the standard University of Wisconsin-Madison Medical Radiation Research Center (UWMRRC) protocol. The dosimeters were read out using a a Harshaw 5500 automated reader (Thermo Fisher Scientific, Inc., Waltham, MA). Additional details about TLD annealing and readout are provided by Nunn et al. and Reed et al. [25, 26] The dose-rate constant analog for the CivaDot using TLD measurements in a PMMA phantom can be determined with the application of Equation 2:

$$\frac{(\dot{D}_{\text{water}})^{\text{CivaDot}}_{\text{water}}}{S_{\text{K}}} = \frac{\lambda}{S_{\text{K}}.(e^{-\lambda t_1} - e^{-\lambda t_2})} \cdot (M_{\text{TLD}})^{\text{CivaDot}}_{\text{phantom}} \cdot CR \cdot IEC \cdot PDC \tag{2}$$

where the notation is $(X_{\text{material}})^{\text{Source}}_{\text{Medium}}$, D is dose, M is charge reading, λ is ^{103}Pd decay constant, t_1, t_2 are start and stop irradiation times respectively, CR is the calibration ratio, IEC is the the intrinsic-energy correction, and PDC refers to the phantom/detector correction. The dose and the charge reading components of this equation can be described as:

- $(M_{\text{TLD}})^{\text{CivaDot}}_{\text{phantom}}$ refers to the in-phantom measurement.
- CR = $\frac{(D_{\text{water}})^{\text{Co-60}}_{\text{Cal}}}{(M_{\text{TLD}})^{\text{Co-60}}_{\text{Cal}}}$ is the calibration ratio.
- IEC = $(\frac{(D_{\text{TLD}})^{\text{CivaDot}}_{\text{phantom}}}{(M_{\text{TLD}})^{\text{CivaDot}}_{\text{phantom}}} \cdot \frac{(M_{\text{TLD}})^{\text{Co-60}}_{\text{Cal}}}{(D_{\text{TLD}})^{\text{Co-60}}_{\text{Cal}}})$ refers to the intrinsic-energy correction.
- PDC = $(\frac{(D_{\text{water}})^{\text{CivaDot}}_{\text{water}}}{(D_{\text{TLD}})^{\text{CivaDot}}_{\text{phantom}}} \cdot \frac{(D_{\text{TLD}})^{\text{Co-60}}_{\text{Cal}}}{(D_{\text{water}})^{\text{Co-60}}_{\text{Cal}}})$ is the phantom/detector correction.

Various correction factors have to be calculated to determine the CivaDot DRC analog. The phantom/detector corrections were calculated using MCNP6 simulations of the measurement geometry and a water phantom. For the TLD measurements, additional TLD micro-cubes were irradiated using a ^{60}Co beam to relevant dose-to-water values for calculating the TLD calibration coefficient (cGy/nC). Since there is no consensus DRC analog value for the CivaDot, the most appropriate intrinsic-energy correction values for the TLD measurements are the NIST-matched x-ray beam M40 (effective energy: 19.2 keV, 40 kVp) value reported by Nunn et al.[25] and the ^{103}Pd Best LDR seed Model 2335 value reported by Reed et al.[26] An average of the valued reported by Nunn et al. and Reed et al. was used. The DRC analog was determined for eight CivaDot sources using TLDs in phantom.

2. EBT3 film

The CivaDot dose-rate constant analog was also measured using EBT3 film. The next section describes the calibration procedure and other associated details for the EBT3 film measurement. Equation 2 was adapted for the EBT3 film measurements, and the related correction factors were determined using MCNP6 simulations of the CivaDot source in the measurement setup and in a water phantom. The DRC analog was estimated using the film measurements by evaluating a region-of-interest (ROI) of the same size as the TLD-micro-cube setup slot, 3×3 mm^2. A comparison of the two dosimeters was performed to evaluate the accuracy of an individual dosimeter and also demonstrate the applicability of using EBT3 film for further characterization of the CivaDot dose distribution. The DRC analog for the CivaDot was then determined for eight sources using EBT3 film.

E. CivaDot dose distribution measurements using a film stack phantom

A PMMA phantom was designed to perform dose measurements of the CivaDot using Gafchromic EBT3 films at multiple depths. Figure 3 is an illustration of the PMMA phantom, $20 \times 20 \times 12$ cm^3, used for these measurements. The CivaDot source was placed in the center of the phantom and six EBT3 films with dimensions, 12×12 cm^2, were irradiated simultaneously along its central axis at various depths. Five EBT3 films were placed on the hot side of the source at distances of 1 cm, 2 cm, 3 cm, 4 cm, 5 cm and one on the cold side of the source at a distance of 0.5 cm. For conventional brachytherapy sources, this measurement is usually performed on the source transverse axis. Measurements were performed for three CivaDot sources using the EBT3 film stack setup.

1. EBT3 film calibration and readout

The EBT3 film dosimeters were read out using an EPSON (Nagano, Japan) 10000XL flatbed scanner. Two days prior to each in-phantom measurement, the required EBT3 film were cut from the same batch. The cropped films were pre-scanned six hours before an exposure along with a set of NIST-traceable optical density (OD) filters (Kodak Wratten™ No. 96 polyester neutral density filters). The measured OD values of the NIST-traceable OD filters [individual pixels converted to optical density using a -log(pixel value/65535) function]

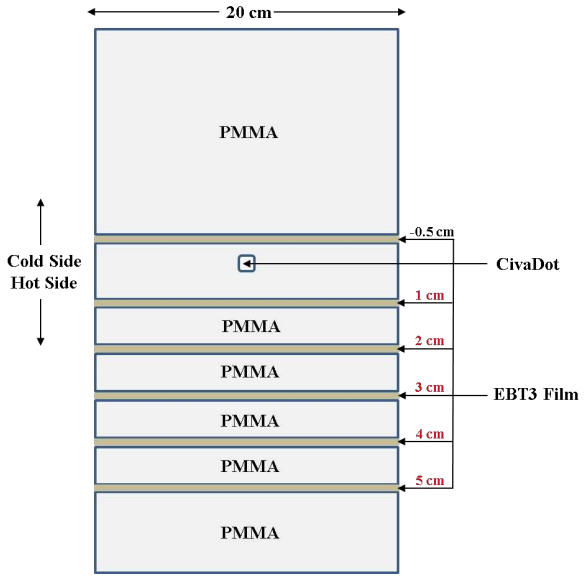

FIG. 3: An illustration of the PMMA film stack phantom setup for the CivaDot dose distribution measurements, using six EBT3 films placed at different depths on the source cylindrical axis. Please note that the illustration is not to scale.

were compared to their actual OD values for every film readout performed. A linear fit function was calculated by fitting the observed and the actual OD values of these filters. The observed individual pixel OD values of the film dosimeters read out were then mapped back to their traceable OD values using the linear fit obtained with the filters. This process mitigates some of the instrument variability between scans as the actual optical density of the filters can be assumed to vary negligibly during the course of the measurements. The films were then read out along with the filters a week after a CivaDot irradiation was performed. Two background films were also used for each measurement, and their net optical density was subtracted from the measured optical density. A calibration curve was determined for the film measurements by irradiating additional films using a NIST-matched M40 x-ray beam (effective energy:19.2 keV, 40 kVp). A total of sixty-two dose-to-water values were used for the calibration curve, with four films irradiated for each dose. The relevant exposure times for the M40 x-ray beam were calculated using a NIST-traceable ionization chamber measurement of the beam air-kerma, and then using a Monte Carlo estimated air-kerma to dose-to-water conversion ratio. Methods outlined by Hammer et al. [27] were followed for the calibration procedure. Figure 4 shows the results of the calibration. A cubic polynomial fit was used to assess the calibration dose value and the measured net

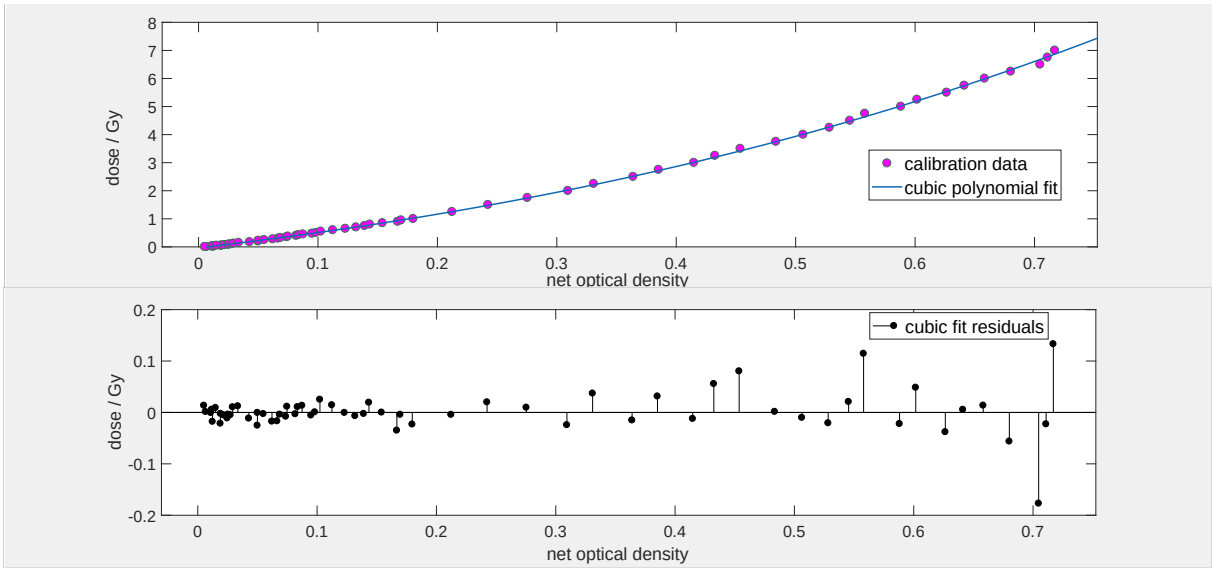

FIG. 4: EBT3 film calibration curve using sixty-two dose-to-water values incorporating different dose levels in a CivaDot in-phantom irradiation. The dose-to-water values ranged from 10 mGy to 7 Gy. A cubic polynomial fit was used to assess the dose and net optical density relationship. A plot of the residuals of the data from the calibration function is also provided in the figure.

optical density relationship. The CivaDot source and the phantom setup were modeled using the MCNP6 code. The phantom/detector corrections were calculated using MCNP6. The intrinsic-energy correction value for this measurement was assumed to be unity based on the findings of Morrison et al. and Chiu-Tsao et al. [28, 29]

2. *Film analysis*

The post-scanning analysis was performed using MATLAB software version R2016a developed by Mathworks Inc. (Natick, MA). The red-channel values were used for all analysis, as the red channel is most sensitive to doses in the range of interest.[30] Once a film was scanned, the individual pixel values were converted to traceable OD filter values and finally, the net OD values for a given film were calculated by subtracting its pre-exposure OD value and the background film OD change from the post-exposure OD value. The net OD values were then converted to absolute dose-to-water values using the calibration curve.

3. Dose difference maps and other TG-43 analog parameters

The measurement setup was simulated using MCNP6. Phantom/detector correction factors were calculated using MC methods. The measured dose distribution values obtained for a given film in phantom were converted to dose-rate to water values. The measured values at different depths were compared to the MC predicted dose distributions at those depths. This comparison was performed using a dose difference map, whereby each pixel of the simulated CivaDot dose distribution was subtracted from the measured CivaDot dose distribution. TG-43 analog dosimetric parameters such as radial dose function analog and 2D anisotropy function analog were also assessed for the measured and the simulated dose distributions. For analysis, an ROI of ± 0.25 mm was set around the relevant dose distribution to calculate a dosimetric parameter.

III. RESULTS

A. NIST WAFAC and UW VAFAC inter-comparison

1. CivaDot energy spectrum comparison

Table I shows the results of the comparison of the CivaDot measured energy spectrum as provided by NIST using a HPGe detector to the energy spectrum calculated for this investigation using MCNP6 simulations of the CivaDot. The measured and the predicted spectrum were normalized to the net counts, yielding relative intensities. Three additional photopeaks were observed in both the measured and the predicted CivaDot energy spectrum when compared to a conventional ^{103}Pd seed spectrum. These spectral peaks (9.7 keV, 11.4 keV, 11.7 keV) correspond to the gold shield fluorescence observed in the source spectrum. All seven photo-peaks for the measured and the predicted spectra agreed to within 1.8%.

2. UW VAFAC correction factors

The correction factors for a CivaDot UW VAFAC Aperture No. 3 were determined by Aima et al.[14] Following the same methods, source-specific correction factors for the CivaDot measurement using the UW VAFAC Aperture No. 2 were calculated for this work.

These factors were calculated using Monte Carlo as outlined in previous publications.[14, 17, 19] NIST determined the source-specific correction factors for the WAFAC CivaDot measurements by applying a combination of empirical, analytical and MC methods as outlined by Seltzer et al.[18] Table II provides the results of the comparison. The CivaDot net correction factor for the two free-air chambers agreed to within 0.7%.

3. CivaDot S_K measurements

A comparison was performed of the S_{K} determination of eight CivaDot sources using the two free-air chambers, as shown in Table III. The S_{K} determined using the UW VAFAC was within 1.1% of the NIST WAFAC values for all eight CivaDot sources with comparable uncertainties, and an average difference of 0.3%.

4. Impact of the aluminum filter on the CivaDot S_K measurements

The impact of the aluminum filter on the UW VAFAC determined CivaDot S_{K} is shown in Table IV. The CivaDot S_{K} determined using the UW VAFAC without the aluminum filter when compared to WAFAC determined values with the presence of an aluminum filter resulted in an agreement to within 0.5% for all three sources measured. There was a noticeable difference in the uncertainty associated with the measurements. The UW VAFAC uncertainty reduced from 1.8% to 1.1%.

B. CivaDot dose-rate constant analog results

Table V presents the results of the dose-rate constant analog determined for the CivaDot with TLD micro-cubes and EBT3 film using eight sources each. The values reported in the columns 2 and 3 of the table present the average measured DRC analog determined with TLD micro-cubes and EBT3 film respectively. The agreement between the TLD measured DRC analog values and MCNP6 predicted DRC analog (0.558 cGy h^{-1} U^{-1}) was within 5% with an average difference of -2.6%. For EBT3 film, all measured values agreed with the MC calculations to within 4% with an average difference of 0.6%. The measured and Monte Carlo weighted DRC analog was determined to be 0.555 cGy h^{-1} U^{-1}.

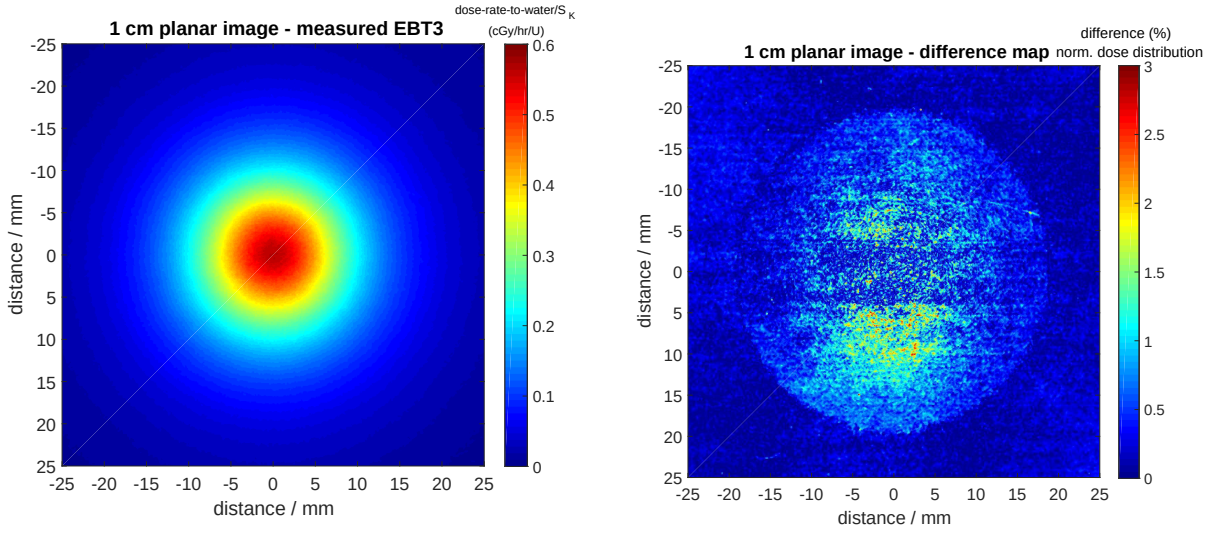

(a) (b)

FIG. 5: a. The results of the CivaDot planar dose-rate distribution measurement using EBT3 film at 1 cm (hot side) from the source along its cylindrical axis normalized to the source air-kerma strength. b. The difference in the measured dose distribution and the predicted dose distribution at 1 cm. Both dose distributions were normalized to the MC maximum dose value.

C. Film stack measurements

The dose rate-to-water distribution normalized to air-kerma strength of a CivaDot measured at a distance of 1 cm (hot side) from the source is shown in Figure 5a. For analysis, the dose-rate distributions normalized to S_K of all three CivaDot sources measured in-phantom using EBT3 film were compared to the MCNP6 predicted dose-rate distribution normalized to S_K at all the six depths. Figure 6 presents the results of the x-profile and the y-profile for the three CivaDot sources measured in-phantom at the 1 cm plane (hot side) as well as the MCNP6 prediction. Figure 5b shows the results of the pixel-by-pixel difference map of the measured and predicted dose distribution of the source at 1 cm depth. As observed in the figure, most differences were within 2% to 3%, with maximum differences up to 5%. On the cold side of the source, the EBT3 measured dose distribution at 0.5 cm agreed with the MC predicted distribution to within 3.5% of the prescribed dose at 1 cm depth.

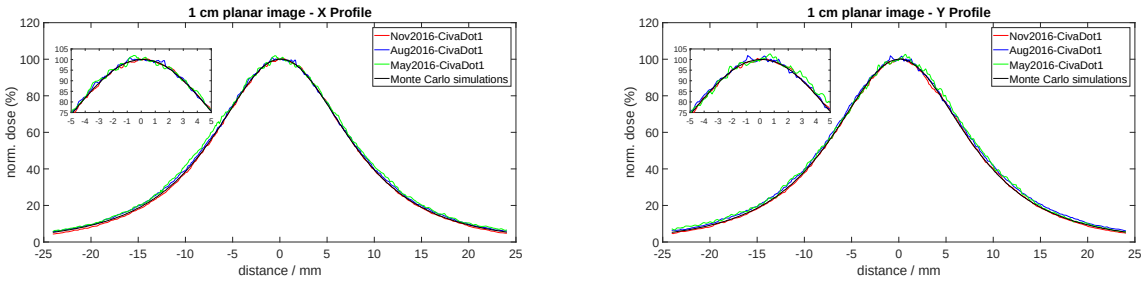

(a) (b)

FIG. 6: The results of the measured profiles for three CivaDot sources as well as Monte Carlo simulated profiles at 1 cm plane (hot side) for (a) x-axis, (b) y-axis. Each curve has been normalized to their respective central-axis dose-rate/S_{K} value.

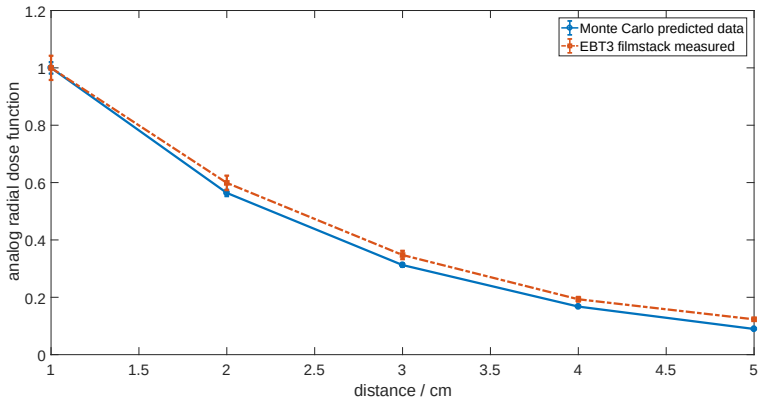

FIG. 7: The radial dose function analog determined for the CivaDot using the EBT3 film stack setup and MCNP6 Monte Carlo simulations.

1. *CivaDot radial dose function analog results*

The radial dose function (RDF) analog was determined for the source based on TG-43 protocol definition adapted to an on-axis definition considering the directionality of the CivaDot. Figure 7 and Table VI present the results of the measured RDF analog and the Monte Carlo predicted RDF analog. Good agreement was observed at 2 cm depth (within 6.3%), with a divergence at deeper depths. On the cold side of the source, the EBT3 measured RDF analog at the depth of 0.5 cm was 0.0462 and the MC predicted RDF analog was 0.0394.

2. CivaDot 2D anisotropy function analog results

Since the measurement setup utilized a stacked geometry, the cylindrical nature of the 2D anisotropy function limits the number of measured data points that can be used for a comparison with Monte Carlo simulations. An ROI of 0.5 mm was set around the intersection of a given polar angle with the film stack planes at set radii. Table VII presents the results of this comparison. Good agreement was observed between the measured and predicted $F(r,\theta)$ ($\leq$6.5%) for distances up to 3 cm.

IV. UNCERTAINTY

The combined (Types A and B) relative standard uncertainty associated with UW VAFAC CivaDot measurements of ^{103}Pd sources was provided in detail by Aima et al. [14] Taking the palladium loading into account, the relative standard uncertainty for the UW VAFAC S_{K} measurement with CivaDots is estimated to be $\sqrt{\sigma_{\mathrm{rep}}^2 + 0.75^2 + 1.62^2}$%, where σ_{rep} is the reproducibility of the free-air chamber measurements as defined by Culberson et al.[17]

The Monte Carlo simulation uncertainty budget is presented in Table VIII for CivaDot DRC analog and RDF analog determination. The Type B uncertainty associated with the simulations were based on the works of Reed et al. [4], Rivard [15], Aima et al.[14] The Type A tally statistics were within 1% for all simulations. An additional component of palladium loading was added as an uncertainty in Monte Carlo predicted values. Dose to water and air-kerma strength simulations were performed with palladium loading of 20% and 80% and a rectangular distribution was assumed for the purposes of uncertainty determination. For the Monte Carlo predicted anisotropy data, uncertainties similar to the RDF analog were observed expect for the palladium loading component. The variation due to palladium loading for the 2D anisotropy function can vary as much as 25% at deeper depths.

The uncertainty associated with measurements performed in phantom using TLD micro-cubes for CivaDot DRC analog determination is presented in Table IX. Typical University of Wisconsin Radiation Calibration Laboratory (UWRCL) uncertainties were assumed for this budget. For EBT3 film measurements, an uncertainty estimation is provided in Table X. The Type A standard deviation of various regions of interest during data analysis was

within 1.5%. The source positioning uncertainty for the measurements was estimated to be within ± 50 μm. The positioning uncertainty for the EBT3 film and TLD measurements was estimated to be within ± 100 μm. The associated uncertainties were calculated using relevant Monte Carlo simulations of the measurement setup and reported in the uncertainty budget of the respective measurements.

V. DISCUSSION

An inter-comparison of the S_K determined for eight CivaDot sources was performed using the UW VAFAC and the NIST WAFAC. The CivaDot energy spectrum was measured by NIST and compared to UW Monte Carlo predicted spectrum. Good agreement was observed in the spectral comparison ($\leq$1.8%), especially considering the fact the Monte Carlo simulations assume a fixed palladium loading. This comparison also validates previous findings published by Aima et al.[14] Gold fluorescence was observed in both the spectra which contributes significantly to the S_K measurement of a CivaDot. A comparison of the S_K determined using the UW VAFAC agreed to within 1.1% of the NIST WAFAC values for all eight CivaDot sources with comparable uncertainties, and an average difference of 0.3%. These results illustrate the good repeatability of the UW VAFAC and NIST WAFAC results and comparable reproducibility of the UW VAFAC measurement to the U.S. national standard. The free-air chamber source-specific correction factors for the CivaDot for the two instruments were comparable. The net correction factor using the two methods was in good agreement (0.7%) as seen in Table II, considering the fact that these are two different free-air chambers. It is also a validation of determining the correction factors using two distinct methodologies. NIST utilizes a combination of empirical, analytical and MC methods approach whereas UW calculates the factors using Monte Carlo methods. It is apparent that the aluminum filter correction is the largest contributor to the overall correction. The aluminum filter attenuates the gold fluorescence present in the CivaDot energy spectrum considerably for both free-air chambers. The use of an aluminum filter for S_K measurement was recommended by the TG-43 report [2] for the exclusion of titanium fluorescence present in conventional LDR sources. However, the CivaDot does not contain a titanium encapsulation and the correction for the aluminum filter attenuation, k_{foil},is about 1.14 to 1.15 for the CivaDot compared to about 1.08 for a conventional ^{103}Pd brachytherapy source. Although

a larger correction does not lead to inaccurate results, the UW VAFAC uncertainty for the measurements takes into account the palladium loading impact (source self-shielding). The intensity of the gold fluorescence changes with the amount of palladium loading. This impacts the k_{foil} factor and once the aluminum filter is removed, this source of uncertainty is mitigated. It was found that the UW VAFAC uncertainty decreases by a factor of about 0.4 as the effect of palladium loading on correction factor uncertainty diminishes.

Dose distribution measurements of the CivaDot were performed using TLD micro-cubes and EBT3 film in a PMMA phantom for eight CivaDot sources to determine the dose rate constant analog. The source dose distribution was also predicted by using Monte Carlo simulations. Good agreement was observed between the two dosimeters and Monte Carlo predicted dose distribution. The average agreement of EBT3 measured DRC analog is within 3.5% of the TLD measured DRC analog for all CivaDot sources measured. This agreement is within the overall uncertainty of the measurements using the two dosimeters. This demonstrates the suitability of using EBT3 film as a dosimeter for absolute dose measurements of LDR brachytherapy sources as TLDs are the standard dosimeter of choice for such measurements. Rivard [15] reported a DRC analog value of 0.579 cGy h^{-1} U^{-1} which is 4.2% different from the DRC analog value determined by this work (0.555 cGy h^{-1} U^{-1}). Potential reasons for disagreement may include differences in the choice of origin and the amount of palladium loading.

A subsequent CivaDot dose distribution measurement was performed using a film stack in a PMMA phantom. EBT3 films were placed at multiple depths in phantom, and measurements were performed for three CivaDot sources. As measurements closer to the source are prone to errors and increased uncertainty, film measurements shallower than 1 cm were not performed. Overall good agreement was observed between EBT3 measured and MC predicted distributions using dose difference maps. The results presented in Figure 6 demonstrate symmetry in source emission across the two axes compared to conventional LDR sources, which may have pronounced anisotropy. Radial dose function analog and 2D anisotropy function analog were also investigated. At depths of 1 cm, 2 cm, 3 cm good agreement was observed for the radial dose function with a slight divergence at deeper depths (4 cm and 5 cm). The absolute dose delivered at depths (4 cm and 5 cm) for a measurement is very small ($\leq$1.5%) compared to the dose prescribed at 1 cm depth, and hence, the measurement uncertainty is much larger. Similar results were seen by Reed et al. [4] when

measuring the RDF for a conventional ^{103}Pd brachytherapy seed and comparing measurements to Monte Carlo data. Rivard's [15] reported RDF analog were in good agreement with the MC RDF analog predicted values. The measured 2D anisotropy function analog agreed to within 6.5% of the MC predicted values for distances up to 3 cm and within 28% for distances of 4 cm and 5 cm. Potential reasons for increased divergence at deeper depths may include the fact that absolute doses were very small at these depths and variation due to palladium loading for the 2D anisotropy function determined by MC can vary as much as 25% at these depths. The limited anisotropy data reported is due to the measurement setup geometry, which is more suitable for a rectangular dosimetric formalism coordinate system. Formulating and proposing an alternative dosimetric formalism instead of an adapted TG-43 formalism can be further researched. A point to consider while using the dosimetric data for clinical purposes is that only the gold shield present in a given CivaDot is visible under computer tomography (CT) imaging, hence it is up to the user to plan accordingly for the post-implant dosimetry, and if possible apply a shift (0.125 mm is the distance from the center of the gold shield to the source origin) to calculate dose more accurately.

Cohen et al.[16] performed an in-phantom measurement using EBT3 film to evaluate the appropriateness of Rivard's results for clinical commissioning of the CivaSheet using relative dosimetry. The dosimetric characterization of a CivaDot as performed in this work will assist in the assessment of the absolute dose distribution of a CivaSheet which is an array of CivaDots.

VI. CONCLUSION

Primary S_{K} measurements of the CivaDot were successfully performed using two different free-air chambers. The investigation assisted in the establishment of a source strength standard for the CivaDot. Dose distribution measurements of the CivaDot performed using TLD micro-cubes and EBT3 films in a PMMA phantom demonstrated good overall agreement with Monte Carlo predicted dose distributions, given the uncertainties. The presence of gold shield x-ray fluorescence was observed in the source energy spectrum and its impact on various aspects of this investigation was evaluated. This work will aid in the eventual realization of a clinically viable dosimetric framework for the CivaSheet by testing the feasibility of using the superposition of an adapted TG-43 dosimetric formalism for a CivaDot.

TABLE I: A comparative analysis of the CivaDot energy spectrum measured by NIST using a HPGe detector and the spectrum calculated using MCNP6 Monte Carlo simulations for this investigation.

Spectral Peak	Energy (keV)	NIST-Measured Spectrum Relative Intensity	UW-MCNP6 Predicted Spectrum Relative Intensity	Difference (%)
Au L_α	9.7	0.0205	0.0167	0.4%
Au L_β	11.4	0.0191	0.0144	0.5%
Au L_β	11.7	0.0059	0.0050	0.1%
Rh K_α	20.1	0.7892	0.8073	-1.8%
Rh K_β	22.7	0.1393	0.1322	0.7%
Rh K_β	23.1	0.0250	0.0209	0.4%
γ	39.7	0.0009	0.0009	0.0%

ACKNOWLEDGMENTS

This work was partially supported by NCI contract (HHSN261201200052C) through CivaTech Oncology, Inc. The authors wish to express their gratitude to John Micka for his continued support throughout the work. We appreciate the feedback and support provided by Dr. Kristy Perez and Dr. Jainil Shah. We also thank the University of Wisconsin Radiation Calibration Laboratory (UWRCL) and the University of Wisconsin Accredited Dosimetry Calibration Laboratory (UWADCL) customers, whose calibrations help support ongoing research at the UWMRRC.

[1] R. Nath, L. L. Anderson, G. Luxton, K. A. Weaver, J. F. Williamson, and A. S. Megooni. Dosimetry of interstitial brachytherapy sources: Recommendations of the AAPM Radiation Therapy Committee Task Group No. 43. *Med. Phys.*, 22(2):209–234, 1995.

[2] M. J. Rivard, B. M. Coursey, L. A. DeWerd, W. F. Hanson, M. S. Huq, G. S. Ibbott, M. G. Mitch, R. Nath, and J. F. Williamson. Update of AAPM Task Group No. 43 report: A revised AAPM protocol for brachytherapy dose calculations. *Med. Phys.*, 31(3):633–674, 2004.

TABLE II: Source-specific correction factors determined for UW VAFAC aperture No. 2 measurements of a CivaDot using MC simulations and NIST WAFAC using a combination of empirical, analytical and MC methods methods.

Source-Specific Correction Factor	Description	NIST WAFAC CivaDot	UW VAFAC CivaDot
k_{sat}	Ion-recombination correction	1.0000	1.0000
k_{hum}	Humidity correction	0.9971	0.9979
k_{stem}	Source-holder correction	1.0000	1.0000
k_{pen}	Aperture-penetration correction	0.9997	0.9985
k_{foil}	Attenuation in aluminum filter	1.1493	1.1400
$k_{\text{att-el}}$	Attenuation through the entrance electrode	1.0000	1.0032
$k_{\text{att-FAC}}$	Attenuation in air from the aperture to the FAC	1.0133	1.0178
$k_{\text{att-SA}}$	Attenuation in air from the source to the aperture	1.0413	1.0383
$k_{\text{int-sca}}$	Internal photon scatter correction	0.9964	0.9917
$k_{\text{ext-sca}}$	External photon scatter correction	0.9945	0.9909
k_{invsq}	Inverse-square correction for aperture	1.0089	1.0086
$\prod k_{\text{corr}}$	Product of correction factors	1.2085	1.2000

[3] M. J. Rivard, W.M. Butler, L.A. DeWerd, M. S.Huq, G.S. Ibbott, A.S. Meigooni, C.S. Melhus, M.G. Mitch, R.Nath, and J.F. Williamson. Supplement to the 2004 update of the AAPM Task Group No. 43 Report. *Med. Phys.*, 34 (6):2187–2205, 2007.

[4] J. L. Reed, M. J. Rivard, J. A. Micka, W. S. Culberson, and L. A. DeWerd. Experimental and Monte Carlo dosimetric characterization of a 1 cm ^{103}Pd brachytherapy source. *Brachytherapy*, 13(6):657–67, 2014.

[5] A. S. Meigooni, H. Zhang, J. R. Clark, V. Rachabatthula, and R. A. Koona. Dosimetric characteristics of the new RadioCoil$^{\text{TM}}$ ^{103}Pd wire line source for use in permanent brachytherapy implants. *Med. Phys.*, 31(11):3095–3105, 2004.

[6] S. Bernard and S. Vynckier. Dosimetric study of a new polymer encapsulated palladium-103 seed. *Phys. Med. Biol.*, 50(7):1493–1504, 2005.

TABLE III: The air-kerma strength inter-comparison results for eights CivaDots using NIST WAFAC and UW VAFAC. The standard uncertainty ('u') for the UW VAFAC was calculated as outlined by Aima et al. [14], and for the NIST WAFAC by Seltzer et al. [18]

NIST Source ID #	UW VAFAC S_K (U)	u (%)	NIST WAFAC S_K (U)	u (%)	Difference (%)
005 A	5.27	1.82	5.27	1.74	-0.1%
005 B	5.30	1.80	5.28	1.78	0.4%
005 C	5.17	1.82	5.16	1.79	0.2%
CSH-010-1	4.22	1.80	4.20	1.69	0.4%
CSH-010-5	4.21	1.82	4.16	1.76	1.1%
CSH-010-7	4.21	1.79	4.20	1.80	0.3%
CSH-010-13	4.13	1.80	4.13	1.75	0.0%
CSH-010-14	4.16	1.80	4.15	1.86	0.2%

TABLE IV: A comparison of the air-kerma strength of three CivaDots determined using the NIST WAFAC with the aluminum filter and the UW VAFAC without the aluminum filter.

NIST Source ID #	UW VAFAC without Al filter S_K (U)	u (%)	NIST WAFAC with Al filter S_K (U)	u (%)	Difference (%)
005 A	5.25	1.05	5.27	1.74	-0.5%
005 B	5.26	1.08	5.28	1.78	-0.5%
005 C	5.14	1.05	5.16	1.79	-0.5%

[7] Z. Wang and N.E. Hertel. Determination of dosimetric characteristics of $OptiSeed^{TM}$ a plastic brachytherapy ^{103}Pd source. *Appl. Radiat. Isot.*, 63(3):311–321, 2005.

[8] F. Abboud, M. Hollows, P. Scalliet, and S. Vynckier. Experimental and theoretical dosimetry of a new polymer encapsulated iodine-125 source - *SmartSeed*: dosimetric impact of fluorescence x rays. *Med. Phys.*, 37(5):2054–2062, 2010.

[9] L. Y. Lin, R. R. Patel, B. R. Thomadsen, and D. L. Henderson. The use of directional interstitial sources to improve dosimetry in breast brachytherapy. *Med. Phys.*, 35(1):240–247,

TABLE V: The average dose-rate constant analog measured using TLD micro-cubes applying the average of Reed et al.'s and Nunn et al.'s intrinsic energy correction factor and Gafchromic EBT3 film for eight CivaDot sources. A comparison with the DRC analog determined using MCNP6 is also provided

Source ID #	Av. Measured DRC analog using TLDs (cGy h^{-1} U^{-1})	Av. Measured DRC analog using EBT3 film (cGy h^{-1} U^{-1})
Sep2015-CivaDot1	0.552	0.555
Sep2015-CivaDot2	0.544	0.553
Sep2015-CivaDot3	—	0.564
CSH-010-13	0.544	0.574
CSH-010-14	0.559	0.543
Dec2015-CivaDot2	0.533	—
Dec2015-CivaDot3	0.531	—
Dec2015-CivaDot4	0.543	—
Dec2015-CivaDot5	0.546	—
May2016-CivaDot1	—	0.580
Aug2016-CivaDot1	—	0.572
Nov2016-CivaDot1	—	0.552
Average DRC analog value	0.544	0.561
Standard deviation	1.7%	2.3%
Average difference from MCNP6 DRC analog	-2.6%	0.6%

2008.

[10] V. Chaswal, B. R. Thomadsen, and D. L. Henderson. Development of an adjoint sensitivity field-based treatment-planning technique for the use of newly designed directional LDR sources in brachytherapy. *Phys. Med. Biol.*, 57(4):963–982, 2012.

[11] R. Nath, L.L. Anderson, J.A. Meli, A.J. Olch, J.A. Stitt, and J.F. Williamson. Code of practice for brachytherapy physics: Report of the AAPM Radiation Therapy Committee Task Group

TABLE VI: Comparison of the average RDF analog measured using EBT3 filmstack (three CivaDot sources) and Monte Carlo simulations.

r	EBT3 measured	MCNP6 predicted		Rivard [15]
(cm)	g_p(r)	g_p (r)	Ratio	g_L (r)
0.5	—	1.3104±0.0262	—	1.3440
1	1.0000±0.0423	1.0000±0.0199	1.0000	1.0000
2	0.5989±0.0253	0.5639±0.0113	1.0621	0.5583
3	0.3475±0.0147	0.3124±0.0062	1.1122	0.3045
4	0.1931±0.0082	0.1676±0.0033	1.1524	0.1640
5	0.1232±0.0052	0.0895±0.0018	1.3760	0.0880

No. 56. *Med. Phys.*, 24(10):1557–1598, 1997.

[12] W. M. Butler, W. S. Bice, Jr., L. A. DeWerd, J. M. Hevezi, M. S. Huq, G. S. Ibbott, J. R. Palta, M. J. Rivard, J. P. Seuntjens, and B. R. Thomadsen. Third-party brachytherapy source calibrations and physicist responsibilities: Report of the AAPM Low Energy Brachytherapy Source Calibration Working Group. *Med. Phys.*, 35(9):3860–3865, 2008.

[13] L.A. DeWerd, J.A. Micka, S.M. Holmes, and T.D. Bohm. Calibration of multiple LDR brachytherapy sources. *Med. Phys.*, 33(10):3804–3813, 2006.

[14] M. Aima, J.L. Reed, L.A. DeWerd, and W.S. Culberson. Air-kerma strength determination of a new directional ^{103}Pd source. *Med. Phys.*, 42(12):7144–7152, 2015.

[15] M. J. Rivard. A directional Pd-103 brachytherapy device: Dosimetric characterization and practical aspects for clinical use. *Brachytherapy*, 16(2):421 – 432, 2017.

[16] G. N. Cohen, K. Episcopia, S. B. Lim, T. J. LoSasso, M. J. Rivard, A. S. Taggar, N. K. Taunk, A. J. Wu, and A. L. Damato Intraoperative implantation of a mesh of directional palladium sources (CivaSheet): Dosimetry verification, clinical commissioning, dose specification, and preliminary experience *Brachytherapy*, 16(6):1257 – 1264, 2017.

[17] W.S. Culberson, L.A. DeWerd, D.R. Anderson, and J.A. Micka. Large-volume ionization chamber with variable apertures for air-kerma measurements of low-energy radiation sources. *Rev. Sci. Instrum.*, 77:015105, 2006.

TABLE VII: Results of 2D Anisotropy function analog measured using the EBT3 film stack phantom and MCNP6

Radial distance (cm)	Polar angle (°)	EBT3 film $F(r,\theta)$	MCNP6 $F(r,\theta)$	Ratio Film/MC
1	0.0	1.0011	0.9996	1.0015
1	120.0	0.0739	0.0698	1.0576
2	0.0	0.9986	0.9993	0.9993
2	60.0	0.9322	0.9431	0.9885
2	104.5	0.1413	0.1329	1.0630
3	0.0	0.9960	0.9994	0.9966
3	48.2	0.9542	0.9625	0.9914
3	70.5	0.8443	0.8951	0.9432
3	99.6	0.1978	0.1859	1.0642
4	0.0	0.9875	1.0003	0.9872
4	41.4	0.8183	0.9790	0.8359
4	60.0	0.7501	0.9354	0.8019
4	75.5	0.6321	0.8701	0.7265
4	97.2	0.1676	0.2312	0.7248
5	0.0	0.9952	0.9997	0.9955
5	36.9	0.8279	0.9803	0.8446

[18] S. M. Seltzer, P. J. Lamperti, R. Loevinger, M. G. Mitch, J. T. Weaver, and B. M. Coursey. New national air-kerma-strength standards for ^{125}I and ^{103}Pd brachytherapy seeds. *J. Res. Natl. Inst. Stand. Technol.*, 108:337–357, 2003.

[19] A.B. Paxton, W.S. Culberson, L.A. DeWerd, and J.A. Micka. Primary calibration of coiled ^{103}Pd brachytherapy sources. *Med. Phys.*, 35(1):32–38, 2008.

[20] A. Colonias, J. Betler, M. Trombetta, G. Bigdeli, O. Gayou, R. Keenan, E. D. Werts, and D. S. Parda. Mature Follow-Up For High-Risk Stage I Non-Small-Cell Lung Carcinoma Treated with Sublobar Resection and Intraoperative Iodine-125 Brachytherapy. *Int. J. Radiat. Oncol. Biol. Phys.*, 79(1):105–109, 2011.

TABLE VIII: Uncertainty budget for Monte Carlo predicted CivaDot TG-43 analog parameters.

	Dose rate constant analog		Radial dose function analog	
Uncertainty parameter	Type A	Type B	Type A	Type B
Palladium loading		2.93%		0.51%
Photon spectrum		0.01%		0.01%
MCNP6 code physics		0.10%		0.14%
μ_{en} / ρ for dose determination		0.87%		1.23%
μ / ρ for photon attenuation		0.31%		0.44%
Tally statistics	1.00%		1.41%	
Quadratic sum	1.00%	3.07%	1.41%	1.41%
Total standard uncertainty		3.23%		2.00%

TABLE IX: Uncertainty budget for CivaDot dose rate constant analog measurement using TLD micro-cubes.

Uncertainty parameter	Type A	Type B
TLD reproducibility	2.00%	
TLD positioning		1.5%
Source positioning		1.00%
Cobalt-60 air kerma rate		0.73%
CivaDot UW S_{K}	0.5%	1.78%
TLD intrinsic energy correction		2.90%
TLD calibration		2.00%
μ_{en}/ρ for corrections		1.23%
μ/ρ for corrections		0.44%
Quadratic sum	2.06%	4.59%
Total standard uncertainty	5.03%	

TABLE X: Uncertainty budget for CivaDot EBT3 film measurements.

Uncertainty parameter	Type A	Type B
Film ROI scanner standard deviation	1.50%	
Scanner and film uniformity		0.60%
Source positioning		1.00%
M40 x-ray air kerma rate		0.45%
CivaDot UW S_{K}	0.5%	1.78%
Film positioning		1.20%
Film intrinsic energy correction		2.30%
Film calibration		1.90%
μ_{en}/ρ for corrections		1.23%
μ/ρ for corrections		0.44%
Quadratic sum	1.58%	4.10%
Total standard uncertainty	4.39%	

[21] Y. Yang and M. J. Rivard. Evaluation of brachytherapy lung implant dose distributions from photon-emitting sources due to tissue heterogeneities. *Med. Phys.*, 38(11):5857–62, 2011.

[22] J.T. Goorley et al, "Initial MCNP6 Release Overview - MCNP6 version 1.0," http://permalink.lanl.gov/object/tr?what=info:lanl-repo/lareport/LA-UR-13-22934, last accessed 01/01/2015.

[23] National Nuclear Data Center, Brookhaven National Laboratory, "Nuclear structure & decay data, Technical Report", www.nndc.bnl.gov/nudat2/, last accessed on 09/07/2014.

[24] M. J. Berger, J. H. Hubbell, S. M. Seltzer, J. Chang, J. S. Coursey, R. Sukumar, and D. S. Zucker. XCOM: Photon cross section database (Version 1.3). [Online] Available: http://physics.nist.gov/xcom (last accessed 16 Nov 2010), National Institute of Standards and Technology, Gaithersburg, MD, 2005.

[25] A. A. Nunn, S. D. Davis, J. A. Micka, and L. A. DeWerd. LiF:Mg,Ti TLD response as a function of photon energy for moderately filtered x-ray spectra in the range of 20 to 250 kVp relative to ^{60}Co. *Med. Phys.*, 35(5):1859–1869, 2008.

[26] J. L. Reed, B. E. Rasmussen, S. D. Davis, J. A. Micka, W. S. Culberson, and L. A. DeWerd. Determination of the intrinsic energy dependence of LiF:Mg,Ti thermoluminescent dosimeters for ^{125}I and ^{103}Pd brachytherapy sources relative to ^{60}Co. *Med. Phys.*, 41(12):122103–1–12, 2014.

[27] C.G. Hammer, B.S. Rosen, J.M. Fagerstrom, W.S. Culberson, and L.A. DeWerd. Experimental investigation of GafChromic EBT3 intrinsic energy dependence with kilovoltage x rays, 137-Cs, and 60-Co. *Med. Phys.*, 45(1):448–459, 2018.

[28] H.Morrison, G.Menon, and R.S. Sloboda. Radiochromic film calibration for low-energy seed brachytherapy dose measurement. *Med. Phys.*, 41(7):072101–1–11, 2014.

[29] S.T. Chiu-Tsao, J.J. Napoli, S.D. Davis, J. Hanley, and M.J. Rivard. Dosimetry for ^{131}Cs and ^{125}I seeds in solid water phantom using radiochromic EBT film. *Appl Rad Isot*, 92:102 – 114, 2014.

[30] V. C. Borca, M. Pasquino, G. Russo, P. Grosso, D. Cante, P. Sciacero, G. Girelli, M. R. La Porta, and S. Tofani. Dosimetric characterization and use of Gafchromic EBT3 film for IMRT dose verification. *Journal of Applied Clinical Medical Physics*, 14(2):158–171, 2013.